

Disintegration of Boron by Fast Neutrons*

B. PETREE,† C. H. JOHNSON,‡ AND D. W. MILLER§
University of Wisconsin, Madison, Wisconsin

(Received May 31, 1951)

The cross section for the $B^{10}(n,\alpha)$ reaction was measured as a function of neutron energy from 0.35 to 2.6 Mev. The cross section was found to lie below the $1/v$ extrapolation of the thermal cross section except at a peak observed at 1.9 Mev. This peak has a width of about 400 kev and a maximum value of 0.53 barn. The total variation of the cross section at the peak is 0.35 barn. The ratio of the number of disintegrations leading to the ground state of Li^7 to the number leading to the excited state increases smoothly from 0.2 at 0.35 Mev to a maximum of 2.3 at 1.9 Mev, and decreases again to 0.8 at 2.6 Mev.

I. INTRODUCTION

STUDIES of the disintegration of boron by neutrons are of interest because of the common use of boron in neutron detectors and shields. An unexpected feature of the $B^{10}(n,\alpha)Li^7$ reaction is that for thermal neutrons there is a strong preference for the Li^7 nucleus to be formed in the 478-kev excited state rather than in the ground state. Hanna¹ found that for thermal neutrons the ratio of the number of disintegrations leading to the ground state of Li^7 to the number leading to the 478-kev excited state is 0.062. An examination of this branching ratio as a function of neutron energy appeared to be useful for the interpretation of the disintegration process. In addition, the flux of neutrons used in the measurement of the branching ratio was determined, so that the $B^{10}(n,\alpha)$ cross section could be obtained at the same time. This cross section was investigated by Bailey *et al.*² at Los Alamos in 1943, but only incomplete results of that work have been published. After the

present experiment was begun, measurements of the branching ratio were published by Bichsel *et al.*³

II. EXPERIMENTAL PROCEDURE

The $B^{10}(n,\alpha)$ disintegration cross section was obtained by determination of the number of disintegration pulses in a proportional counter, the number of B^{10} nuclei in the counter, and the number of neutrons per cm^2 causing the disintegrations. Figure 1 shows the geometrical arrangement of the neutron source and the neutron counters used in this experiment. Fast neutrons were produced by bombarding targets at T with a proton beam B accelerated by the electrostatic generator. The energy of the protons was measured by passing them through a one-meter radius electrostatic analyzer.⁴ A lithium target, evaporated in place on a tantalum backing, was used to provide monoenergetic neutrons in the energy range from 0.35 to 1.30 Mev. Neutrons with energies from 0.95 to 2.65 Mev were obtained using a target which consisted of tritium absorbed in zirconium film on a tungsten backing. The proportional counter, C , with which the $B^{10}(n,\alpha)Li^7$ and $B^{10}(n,\alpha)Li^{7*}$ disintegrations were observed, and the neutron flux monitor M were mounted along lines making equal angles with respect to the axis of the proton beam.

The flux monitor M was a "long counter" of the type developed by Hanson and McKibben.⁵ From 10 kev to 5 Mev, the efficiency of this monitor is nearly independent of neutron energy. By observing the counting rate when a calibrated radium-beryllium neutron source was placed at the position normally occupied by the lithium or tritium target, it was possible to determine the monitor efficiency. A correction was applied to the monitor counting rate for the background of scattered neutrons.

Because of the necessity of distinguishing between disintegrations leading to the ground state of Li^7 and those leading to the excited state, special care was required in the construction of the BF_3 proportional counter. In the most common design of simple proportional counters the small center wire is supported at

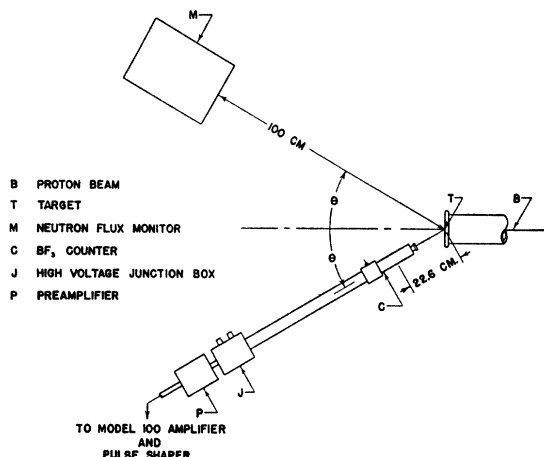


FIG. 1. Experimental arrangement for observing boron disintegrations and measuring neutron flux.

* Work supported by the AEC and the Wisconsin Alumni Research Foundation.

† Now at National Bureau of Standards, Washington, D. C.

‡ Now at Oak Ridge National Laboratory, Oak Ridge, Tennessee.

§ AEC Predoctoral Fellow.

¹ G. C. Hanna, *Phys. Rev.* **80**, 530 (1950).

² C. L. Bailey, *et al.*, (unpublished); quoted by R. K. Adair, *Revs. Modern Phys.* **22**, 249 (1950).

³ Bichsel, Halg, Huber, and Stebler, *Phys. Rev.* **81**, 456 (1951).

⁴ Warren, Powell, and Herb, *Rev. Sci. Instr.* **18**, 559 (1947).

⁵ A. O. Hanson and J. L. McKibben, *Phys. Rev.* **72**, 673 (1947).

each end by larger wires. The supporting wires are usually enough larger than the center wire that the field at their surfaces is too small to produce gas multiplication. Only the ions which are collected on the small wire undergo gas multiplication and produce full-size pulses. For such an arrangement the active volume is about as long as the small wire. This simple construction has two faults which made it undesirable for use in the measurements reported here. The active volume is not easy to determine accurately because of the distortion of the field lines near the ends of the small wire. In addition, a spread in pulse size occurs because the gas multiplication gradually diminishes to unity near the ends of the wire.

These undesirable end effects associated with the termination of the center wire were eliminated by a design similar to that described by Cockroft and Curran.⁶ Figure 2 shows a cross-sectional view of the counter used in the present experiment. A thin-walled guard sleeve was installed concentric to the center wire at each end and maintained at an intermediate voltage appropriate to its radius. If the guard sleeves were sufficiently long, the electric field at the surface of the wire would be uniform and radial along its entire exposed length. For shorter lengths of guard sleeve, however, the field at the end of the sleeve is rather sensitive to the radius of the annular gap which separates the guard sleeve from the grounded shell of the counter.

The optimum radius of this gap was determined from electrolytic tank studies of an enlarged model of the counter. It was found that with the gap placed as in Fig. 2 the equipotential lines between counter wall and guard sleeves are straight and parallel at a distance of one-half inch from the gap. One-half inch is, therefore, a sufficient length of guard sleeve to make the field at the wire uniform and radial, provided the wire is smooth, round, and properly centered. Under these conditions the active volume is simply determined by the exposed length of the wire. There is still a spread in the pulse height for a given initial ionization in this counter because of wall effects and the properties of the filling gas, but the serious spread caused by non-uniformity of the field was largely eliminated.

A typical pulse-height distribution curve obtained for slow neutrons is shown in Fig. 3. The groups of pulses at 2.30 and 2.78 Mev, representing $B^{10}(n,\alpha)Li^{7*}$ and $B^{10}(n,\alpha)Li^7$ disintegrations in the gas,⁷ are sufficiently well resolved that their respective numbers can be determined with little ambiguity. Disintegrations of boron atoms deposited on the wall of the counter are responsible for the groups of pulses at 1.46 and 0.84 Mev. Since the alpha-particle and the Li^7 nucleus are emitted in opposite directions, only one of them can enter the active volume of the counter when a disintegration occurs on the wall. The alpha-particle and the

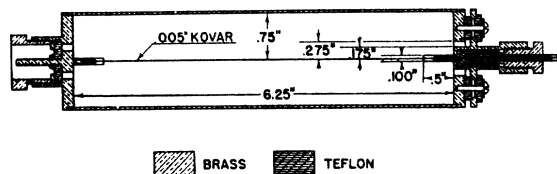


FIG. 2. Proportional counter for observing boron disintegrations.

Li^7 nucleus receive 7/11 and 4/11 of the disintegration energy, respectively. For disintegrations producing Li^7 in the excited state ($Q=2.30$ Mev), the alpha-particle and Li^7 energies are 1.46 and 0.84 Mev. For the less frequent disintegrations producing Li^7 in the ground state ($Q=2.78$ Mev), the alpha-particle and Li^7 energies are 1.77 and 1.01 Mev. The 1.77- and 1.01-Mev pulses are not sufficiently numerous to appear distinctly in Fig. 3.

While a large pressure of BF_3 is desirable for the sake of a large counting rate, it was found that good pulse-height resolution could not be obtained with BF_3 at a pressure greater than two inches of mercury. A deterioration of the resolution with time was also noticed. Fowler and Tunnicliffe⁸ have attributed the deterioration to the formation of a gas with strong electron attachment properties by the chemical action of BF_3 on traces of impurities. Because of this effect, it was necessary to refill the counter several times during the course of the experiment. A useful life of two or three days was obtained by limiting the BF_3 pressure to one inch of mercury.

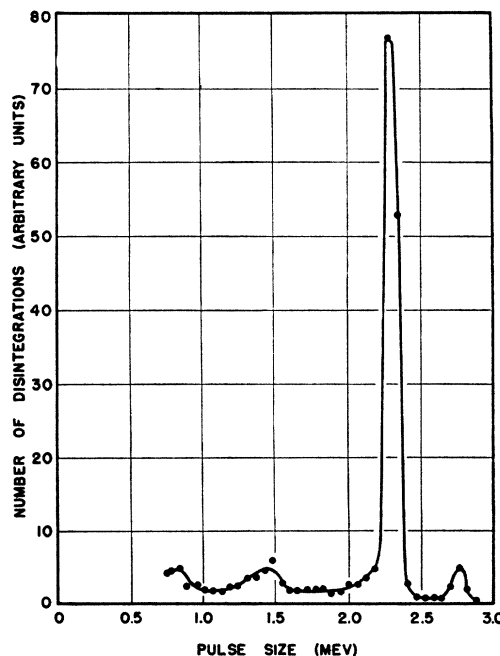


FIG. 3. Pulse-height distribution for slow neutron disintegration of boron.

⁶ A. L. Cockroft and S. C. Curran, *Rev. Sci. Instr.* **22**, 37 (1951).
⁷ Hornyak, Lauritsen, Morrison, and Fowler, *Revs. Modern Phys.* **22**, 291 (1950).

⁸ I. L. Fowler and P. R. Tunnicliffe, *Rev. Sci. Instr.* **21**, 734 (1950).

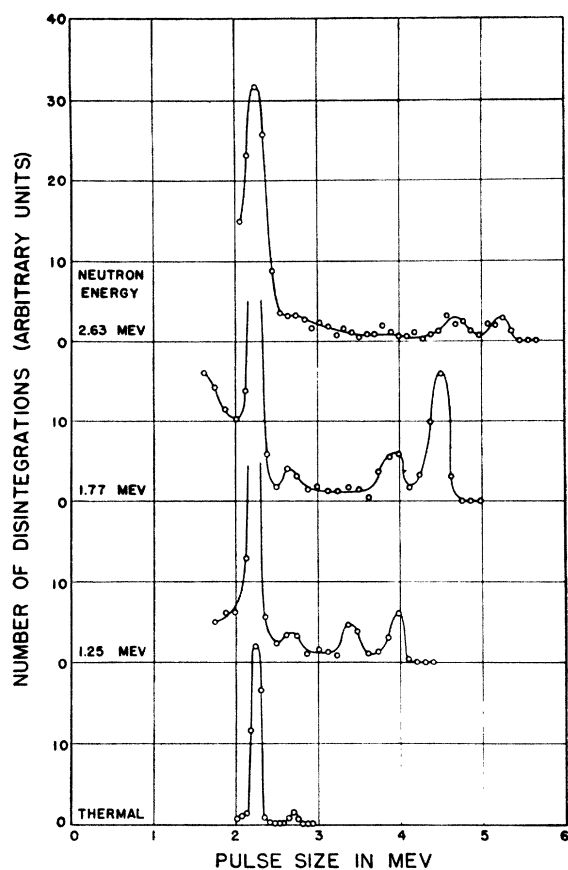


FIG. 4. Typical pulse-height distributions for $B^{10}(n,\alpha)$ reaction. Slow neutron disintegration pulses are at 2.30 and 2.78 Mev. Fast neutron disintegration pulses are at 2.30 and 2.78 Mev plus the neutron energy.

BF_3 enriched in the B^{10} isotope was used to increase the counting rate. The isotopic composition of the enriched BF_3 was not known accurately. To determine the number of B^{10} atoms in the active volume of the counter, the counting rate was measured both with ordinary BF_3 (18.8 percent B^{10}) and enriched BF_3 . For these measurements the counter and a Ra-Be neutron source were placed in reproducible positions in a large paraffin cylinder. The counting rate in this standard geometry was determined immediately after each filling with enriched BF_3 , and was measured occasionally thereafter until a fresh filling was needed to restore the resolution. The counting rate decreased slowly with time; in the worst instance the final rate was 85 percent of the initial rate measured three days earlier. This decrease in counting rate was probably caused largely by the gradual deposition of boron on the walls of the counter. Although the boron in the enriched BF_3 was supposed to be 96 percent B^{10} , the standard geometry measurements indicated only 50 to 60 percent.

The best pulse-height resolution was obtained with argon at 35 psi as the stopping gas. At this relatively low pressure the wall effect is appreciable. A correction

for this effect was estimated by the method described by Rossi and Staub.⁹ For thermal neutrons it was calculated that 12 percent of the (n,α) pulses would be reduced in size because of wall effect, in agreement with the experimental results. The wall effect correction at higher neutron energies was found by the same method, taking into account the increased range of the alpha-particles.

In order to make certain that neutron reactions with argon were not producing an appreciable number of pulses, the counter was filled with pure argon at 35 psi and exposed to fast neutrons at several energies covering the range of the experiment. The number of pulses observed in this way was less than 5 percent of the number observed with argon and BF_3 .

A closely fitting cadmium shield was installed on the counter to reduce the number of disintegration pulses caused by the background of thermal neutrons. The background of epithermal neutrons scattered from the floor still gave an appreciable number of disintegration pulses at 2.30 and 2.78 Mev. These pulses were useful for calibrating pulse size in terms of disintegration energy.

Disintegration pulses from the proportional counter were amplified with a Model 100 amplifier and recorded photographically.

III. RESULTS

Figure 4 gives the pulse-height distributions obtained at several neutron energies. The bottom curve, obtained with thermal neutrons, shows the two groups of pulses at 2.30 and 2.78 Mev which correspond to the processes $B^{10}(n,\alpha)Li^{7*}$ and $B^{10}(n,\alpha)Li^7$. The strong preference for $B^{10}(n,\alpha)Li^{7*}$ is evident. Approximately equal fluxes of fast neutrons were used to obtain the other three curves in Fig. 4. Groups of pulses at 2.30 and 2.78 Mev on these curves were caused by the background of epithermal neutrons. The disintegrations caused by fast neutrons appear at 2.30 and 2.78 Mev plus the neutron energy. At 1.25-Mev neutron energy the reactions $B^{10}(n,\alpha)Li^{7*}$ and $B^{10}(n,\alpha)Li^7$ have about equal probability; at 1.77 Mev $B^{10}(n,\alpha)Li^7$ predominates, in contrast to the result at thermal energy; at 2.63 Mev the two processes are again about equally probable. Large variations in the (n,α) disintegration cross section can be seen on these curves; the relatively large number of fast neutron disintegrations at 1.77 Mev means a relatively large cross section at that neutron energy.

It will be noted in Fig. 4 that an appreciable number of intermediate size pulses was observed, smaller than the fast neutron pulses and larger than those produced by the slow neutron background. These intermediate size pulses are about twice as numerous as would be expected from wall effect. The pulses are too large to have been caused by neutron reactions with B^{11} or F^{19} , all of which are endothermic, or by the reactions

⁹ B. B. Rossi and H. H. Staub, *Ionization Chambers and Counters* (McGraw-Hill Book Company, Inc., New York, 1949), p. 236.

$B^{10}(n,p)Be^{10}$ ($Q=+0.2$ Mev) or $B^{10}(n,2\alpha)H^3$ ($Q=+0.3$ Mev). An appreciable number of these pulses was probably caused by neutrons scattered inelastically from the floor and from the walls of the counter.

Twenty pulse-height distributions were taken at various neutron energies from 0.35 to 2.63 Mev. The pulses produced by fast neutrons were found to increase in size linearly with neutron energy. Below 0.35-Mev neutron energy the cross section could not be measured because the fast and slow neutron disintegration pulses overlapped.

Figure 5 shows the cross sections and branching ratios determined in this experiment. Neutrons from the $Li^7(p,n)$ reaction were used to obtain the data represented by solid circles. Open circles denote data obtained with $T(p,n)$ neutrons. The statistical uncertainty is indicated by the vertical bars. It should be emphasized that the cross section plotted in the upper part of Fig. 5 is for normal boron, which contains only 18.8 percent B^{10} .

Aside from the statistical uncertainty, the accuracy of the cross section is limited by the precision with which the neutron fluxes and the quantity of B^{10} in the counter were determined. The quantity of B^{10} depends on the BF_3 pressure and the standard geometry measurements, both of which were accurate to about 5 percent. A determination of the strength of the Ra-Be source was made by comparison at the Argonne National Laboratory with a standard source whose

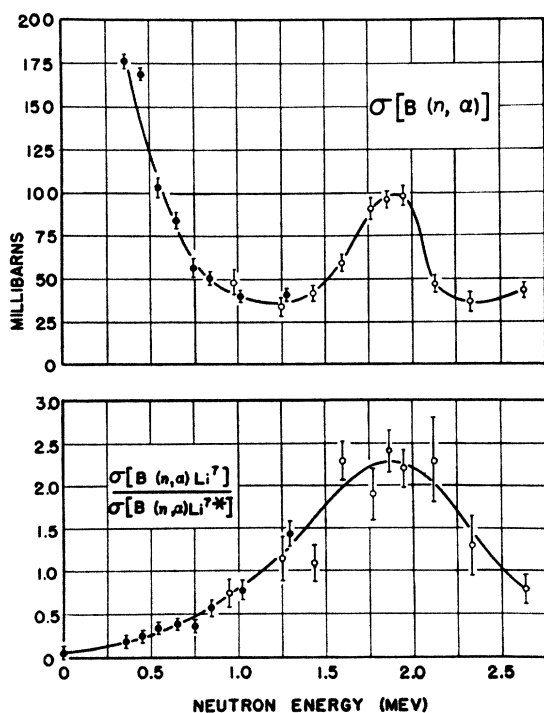


FIG. 5. Upper curve, (n,α) disintegration cross section of ordinary boron. Lower curve, ratio of the number of disintegrations leading to the ground state of Li^7 to the number leading to the 478-kev excited state.

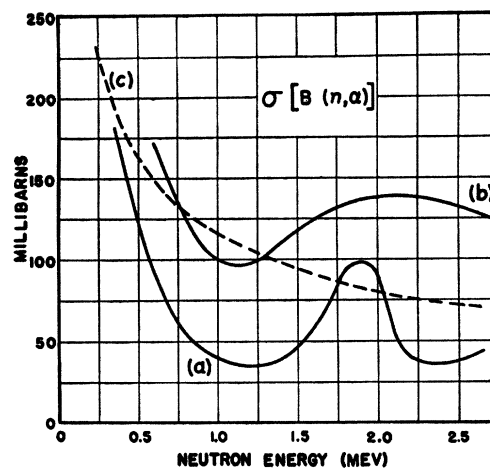


FIG. 6. The (n,α) cross section of ordinary boron. (a) Present experiment; (b) Bailey *et al.* (reference 2); (c) $1/v$ extrapolation of the slow neutron cross section determined by Sutton *et al.* (reference 10).

strength is believed to be known to 7 percent. The efficiency of the monitor was probably equal, within 5 percent, for both Ra-Be neutrons and the fast neutrons with which the cross sections were observed. Background corrections may be in error by as much as 10 percent. The combined effect of these uncertainties is estimated to be about ± 25 percent of the cross sections.

It is difficult to estimate the accuracy of the branching ratio measurements. The total uncertainty is somewhat greater than the statistical uncertainty indicated in the lower part of Fig. 5 because of the imperfect resolution of the $B^{10}(n,\alpha)Li^7$ and $B^{10}(n,\alpha)Li^{7*}$ pulses. The pulse height distribution curves of Fig. 4 indicate rather clearly, however, that the ratio is about two at 1.77-Mev neutron energy, and that it is about one at neutron energies of 2.63 and 1.25 Mev.

In this experiment, the uncertainty in neutron energy is caused almost entirely by the uncertainty in the angle of observation, which was less than 3 degrees. The energy uncertainty is nearly proportional to the square root of the neutron energy, and at 1.9 Mev is about 60 kev.

Figure 6 shows the (n,α) cross sections determined in the present experiment, the cross sections determined by Bailey *et al.*² at Los Alamos, and the $1/v$ extrapolation of the cross sections determined by Sutton *et al.*¹⁰ for slow neutrons.

No information is available regarding the epithermal neutron background for the work of Bailey *et al.*, nor how or if a correction for such a background was applied. If no background correction was applied, it seems likely that their cross sections are too large. In the present experiment only pulses of a size consistent with the energy of the direct neutron flux were counted

¹⁰ Sutton, McDaniel, Anderson, and Lavatelli, *Phys. Rev.* **71**, 272 (1947).

TABLE I. Reduced widths assuming a single level at 1.9 Mev having $J=11/2$.

Particle	L	Particle width	$\gamma^2 \times 10^{13}$	$\gamma^2 \div \frac{3}{2} \frac{\hbar^2}{Ma}$
Neutron	2	$\frac{1}{2}\Gamma$	1.14	0.08
Alpha	5	$\frac{3}{2}\Gamma$	5.4	1.2

in calculating the cross section, whereas in the measurements of Bailey *et al.*, no pulse-height analysis was made.

Bichsel *et al.*³ have measured the branching ratio at five neutron energies from 0.5 to 3.9 Mev, and obtained results similar to the lower part of Fig. 5. They found a maximum value of two for the branching ratio at a neutron energy of 2.9 Mev, whereas the present experiment indicates that the maximum occurs at 1.9 Mev. The reason for the discrepancy is not clear.

It will be noted in Fig. 5 that the maxima in the branching ratio and the $B(n,\alpha)$ cross section appear to coincide at 1.9 Mev. A satisfactory interpretation of this effect has not been found.

IV. DISCUSSION

The peak in the disintegration cross section at 1.9-Mev neutron energy indicates the presence of one or more levels in the B^{11} compound nucleus. This peak has a width of 400 kev, which is more than four times the experimental neutron energy spread. The rise in the cross section at the peak is caused almost entirely by the increased number of disintegrations leading to the ground state of Li^7 .

For an isolated resonance, the maximum value of the disintegration cross section given by the Breit-Wigner formula is

$$\sigma_a^R = [(2J+1)/2(2I+1)](4\pi/k^2)\Gamma_n\Gamma_a/\Gamma^2. \quad (1)$$

I and J are the angular momenta of the target and compound nuclei in units of \hbar , k is the wave number for neutrons of resonance energy, and Γ_a and Γ_n are the partial widths for alpha-particle and neutron emission. Γ is the total width, which is observed experimentally, and is the sum of the partial widths for all possible modes of decay of the compound nucleus. In expression (1), σ_a^R denotes the maximum value of the (n,α) cross section for the isotope B^{10} . Figure 5 shows clearly that the peak in the disintegration cross section is not isolated as required by Eq. (1). Broad resonances above and below 1.9 Mev may contribute appreciably at 1.9 Mev and prevent the disintegration cross section from approaching zero on either side. Under the assumption that neighboring levels do not interfere, then, σ_a^R is taken to be the change in the B^{10} disintegration cross section at the peak rather than its maximum value. When defined in this way, σ_a^R is obtained by dividing the change in the cross section at the peak in Fig. 5 by 0.188, the isotopic abundance of B^{10} in normal boron.

A lower bound for J can be obtained from Eq. (1)

if it is assumed that $\Gamma_n = \Gamma_a = \Gamma/2$. However, recent measurements by Bockelman *et al.*¹¹ at this laboratory have shown that the rise in total cross section at 1.9 Mev is no larger than the rise in the disintegration cross section. From this it is concluded that Γ_n is considerably smaller than Γ_a . This result requires that J must be at least $11/2$ in order to satisfy Eq. (1). To produce a compound nucleus with that angular momentum, incoming neutrons with at least two units of orbital angular momentum would be necessary. If one assumes a spin of $1/2$ for the excited state of Li^7 , and that the ground state and the excited state have the same parity, the alpha-particles emitted in the disintegration processes must be emitted with five units of angular momentum.

An estimate of the upper limit for the angular momentum of the compound nucleus can be obtained from an examination of the reduced widths for the various modes of decay. The width for the emission of a particle, s , can be written¹²

$$\Gamma_s = 2kT_L\gamma_s^2,$$

where k is the wave number of the emitted particle, T_L is the barrier penetration factor for a particle with orbital angular momentum L , and γ_s^2 is called the reduced width. If the emitted particle is charged, T_L is the coulomb barrier penetration factor for particles of orbital angular momentum L . For neutrons, T_L , the centrifugal barrier penetration factor, can be calculated explicitly.¹³ The reduced widths for the emission of various particles from a given level of a compound nucleus are not expected to differ greatly.¹⁴ A reduced width cannot exceed $3\hbar^2/2Ma$, where M is the reduced mass of the emitted particle, and a is the radius of interaction of the emitted particle and the residual nucleus.¹⁴ Since the barrier penetration factors decrease with increasing L , the calculated value of the reduced width increases as larger values of L are assumed. The limit on the reduced width thus imposes an upper limit on L and hence on J .

Table I gives the reduced widths, in units of 10^{-13} Mev-cm, calculated for neutron and alpha-particle emission, assuming that $J=11/2$. For these calculations, the ratio Γ_n/Γ was taken to be $\frac{1}{2}$. A larger neutron width would not be compatible with the measurements of total cross section and absorption cross section. The radius of interaction for neutron emission was taken as 4.5×10^{-13} cm, and for alpha-particle emission, 5.2×10^{-13} cm. These numbers are the sums of the radii of the emitted particle and the residual nucleus in the two cases. The radii were assumed to be $1.43A^{\frac{1}{3}} \times 10^{-13}$ cm, where A is the mass number.

Thus, a value of $11/2$ for J , which is required to account for the total cross section and disintegration

¹¹ Bockelman, Miller, Adair, and Barschall, Phys. Rev. **84**, 69 (1951).

¹² R. K. Adair, Revs. Modern Phys. **22**, 249 (1950).

¹³ Feshbach, Peaslee, and Weisskopf, Phys. Rev. **71**, 145 (1947).

¹⁴ E. P. Wigner, Am. J. Phys. **17**, 99 (1949).

cross-section data, leads to a reduced width for alpha-particle emission which is 20 percent larger than the theoretical maximum. Although the assumption of other processes besides neutron and alpha-emission may decrease Γ_α , the reduced width for alpha-particle emission will not become smaller. For if Γ_α is reduced while Γ_n and Γ remain fixed, J must be increased to satisfy Eq. (1). The net effect then is to increase rather than to reduce the calculated reduced width. Hence, a state of the compound nucleus with $J=11/2$ does not seem possible.

The single-level scheme is not definitely excluded, however, because under certain rather special conditions the total cross section can show only a small variation in the neighborhood of a resonance with a large neutron width. Although a J value of $7/2$ is somewhat beyond the limit of the experimental uncertainty of the disintegration cross-section data, such a state of the compound nucleus can provide an explanation for the absence of a prominent resonance in total cross section at 1.9 Mev. A state with $J=7/2$ can be produced by both S - and D -neutrons. It is possible for a dip rather than a rise in the scattering cross section for S -neutrons to occur at the resonance energy because of destructive interference between resonance and potential scattering. Since the S -wave potential phase shift for 1.9-Mev neutrons is in the neighborhood of 90 degrees, such a dip would be expected.¹⁵ For D -neutrons, however, the potential phase shift is too small to produce any appreciable interference, and a peak would occur at resonance. If one assumes S - and D -neutron widths of 0.1 and 0.4 of the total width, partial cancellation would reduce the variation in scattering cross section at the 1.9-Mev resonance to about 0.05 barn. In that case total cross-section measurements would be expected to show only the effect of processes other than elastic scattering.

With this scheme, therefore, it is possible to reconcile a large neutron width with the experimental fact that the total cross-section peak is no larger than the (n,α) peak. A J value of $7/2$ permits the alpha-particles to be emitted with only three units of orbital angular momentum. The reduced neutron and alpha-particle widths are tabulated in Table II in units of 10^{-13} Mev-cm, together with the assumed angular momenta of the emitted particles, the assumed widths for the processes, and the ratios of the reduced widths to the theoretical maxima. The two alpha-particle widths

TABLE II. Reduced widths assuming a $J=7/2$ level at 1.9 Mev formed by both S - and D -neutrons.

Particle	L	Particle width	$\gamma^2 \times 10^{13}$	$\gamma^2 \frac{3}{2} \frac{\hbar^2}{Ma}$
S neutron	0	0.1 Γ	0.07	0.0048
D neutron	2	0.4 Γ	1.8	0.12
Long-range alpha	3	0.33 Γ	0.27	0.058
Short-range alpha	3	0.17 Γ	0.13	0.028

were taken in the ratio of two to one, as is indicated by the branching ratio at 1.9 Mev.

The reduced widths in this scheme are not unreasonable, and there is fair agreement with the disintegration cross-section data. With $J=7/2$, and $\Gamma_n = \Gamma_\alpha = \Gamma/2$, as has been assumed in Table II, the height of the (n,α) peak calculated from Eq. (1) is 30 percent less than the measured height. The percentage difference between calculated and observed heights will increase, however, if Γ_n and Γ_α are reduced to allow for other processes. The somewhat artificial scheme summarized in Table II is the most nearly satisfactory single-level interpretation of the peak at 1.9 Mev.

It is more plausible to assume that the peak is caused by two or more closely spaced levels. With two levels to contribute to the disintegration cross section, small J -values are adequate to account for the height of the absorption peak. For small J -values, the reduced widths are found to be reasonably small. Provided one level is produced by S -neutrons, the small height of the total cross-section peak can be explained as before. Because of the many parameters available in the two-level scheme, the levels cannot be uniquely specified.

A surprising result of this experiment is the apparent scarcity of levels from 0.35- to 2.63-Mev neutron energy. The corresponding interval in the excitation energy of the B^{11} nucleus is 11.74 to 13.81 Mev.⁷ In this interval of 2.07 Mev, only the one peak at 1.9 Mev was observed. From an investigation of the $B^{10}(d,p)$ reaction, Van Patter *et al.*¹⁶ list ten excited states in B^{11} below 10 Mev, with a marked trend toward closer spacing at higher excitation energies. In the 2.52-Mev region between 6.76 and 9.28 Mev, seven levels were observed. The interval between 10.2 and 11.46 Mev has not been explored. A level density higher than that found previously around 9 Mev might be expected in the range of energies covered in the present measurement, adding to the plausibility of the two-level interpretation of the (n,α) disintegration peak at 1.9 Mev.

¹⁵ M. R. MacPhail, Phys. Rev. 57, 669 (1940).

¹⁶ Van Patter, Buechner, and Sperduto, Phys. Rev. 82, 248 (1951).